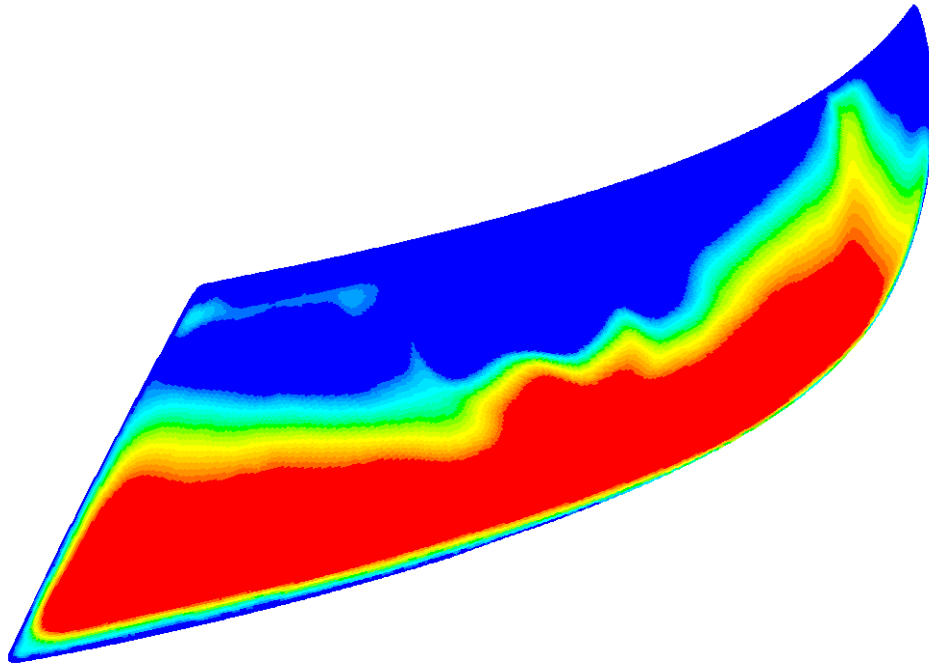


# CHALMERS



## CFD Modelling of Headlamp Condensation

*Master's Thesis in Automotive Engineering*

JOHAN BRUNBERG

MIKAEL ASPELIN

Department of Applied Mechanics  
*Division of Vehicle Engineering and Autonomous Systems*  
CHALMERS UNIVERSITY OF TECHNOLOGY  
Göteborg, Sweden 2011  
Master's Thesis 2011:34



MASTER'S THESIS 2011:34

# CFD Modelling of Headlamp Condensation

Master's Thesis in *Automotive Engineering*

JOHAN BRUNBERG

MIKAEL ASPELIN

Department of Applied Mechanics  
*Division of Vehicle Engineering and Autonomous Systems*  
CHALMERS UNIVERSITY OF TECHNOLOGY  
Göteborg, Sweden 2011

CFD Modelling of Headlamp Condensation  
Master's Thesis in *Automotive Engineering*

JOHAN BRUNBERG  
MIKAEL ASPELIN

© JOHAN BRUNBERG, MIKAEL ASPELIN, 2011

Master's Thesis 2011:34  
ISSN 1652-8557  
Department of Applied Mechanics  
Division of Vehicle Engineering and Autonomous Systems  
Chalmers University of Technology  
SE-412 96 Göteborg  
Sweden  
Telephone: + 46 (0)31-772 1000

Cover:  
Outer lens of the Saab 9-3 headlamp, showing contours of condensation film thickness

Chalmers Reproservice / Department of Applied Mechanics  
Göteborg, Sweden 2011

# ABSTRACT

An automotive headlamp is exposed to thermal variations together with low air exchange. The possibility of humidity entering the headlamp will therefore increase the risk for condensation to form on the lamps inner surface. The automotive industry today is highly competitive and tends to focus more on reducing costs together with consumers demanding more advanced features and styling characteristics such as transparent optical plastics and low energy emitting lamps. This will cause problems if dew is formed and visible from the outside. Physical testing and validation are not available until late in the development process and are expensive to perform. Therefore it is of great importance for the car manufacturer to be able to simulate the risk for condensation early in the design stage and thereby also reduce the cost.

Thus, the goal in this thesis is to develop a numerical method with help of Computational Fluid Dynamics (CFD) that will predict if and where condensation will form in an automotive headlamp.

Engineers at Saab Automobile AB today rely fully on physical testing obtained from climate tunnel experiments, pushing the headlamp to its limits during extreme weather conditions and thereby visualizing the behavior of condensation. The purpose is to evaluate if a numerical method is possible to include the condensation phenomena and compare the dew pattern formed during the climate tunnel experiments to the numerical model.

Furthermore, a numerical model was successfully developed and predictions of condensation were found to be within an acceptable range, though with a slight deviation. It was also found that the possible source of deviation may lie in how scattering of light is treated in the numerical model, foremost the boundary conditions governed by it. Hence, further work is imposed to solve this.

Key words: Headlamp, Condensation, CFD



# Contents

ABSTRACT	I
CONTENTS	III
ACKNOWLEDGEMENTS	V
NOMENCLATURE	VII
1 INTRODUCTION	1
1.1 Background	1
1.1.1 Headlamp design	3
1.1.2 Physical approach	5
1.2 Objectives	6
1.3 Delimitations	6
2 METHODOLOGY	7
2.1.1 Pre-processing	7
2.1.2 Solving	7
2.1.3 Post-processing	7
3 NUMERICAL SIMULATIONS	8
3.1 Theory	8
3.1.1 Convection	9
3.1.2 Conduction	10
3.1.3 Radiation	10
3.1.4 Condensation	12
3.1.5 Fluid dynamics	15
3.2 Numerical Setup	16
3.2.1 Computational grid	16
3.2.2 Solution Process	24
4 RESULTS	26
4.1 Temperature distribution	26
4.2 Velocity distribution	28
4.3 Film thickness	30
5 CONCLUSION	31
6 RECOMMENDATIONS	32
7 REFERENCES	33
8 APPENDIX A	35



## Acknowledgements

In this study, a numerical method that predicts were formation of condensation occurs for an Automotive headlamp has been developed. The thesis has been carried out from January 2011 to June 2011.

The project was carried out at the Aero & Thermal CAE group at Saab Automobile AB in Trollhättan, Sweden.

First of all we would like to thank our supervisor Mark Saukkonen for his support and expertise. We would also like to thank the rest of the Aero & Thermal group, Anders Björtn, Robin Larsson, Tobias Persson and Jesper Marklund for their support during the project.

We would also like to thank Erik Preihs at SAAB Automobile for providing his expertise and previous work regarding the headlamp.

We would also like to thank Professor Lennart Löfdahl at *Chalmers Institute of technology* for the possibility to do this thesis work.

All simulations have been carried out at the Saab Aero & Thermal CAE group. We would also like to thank Torbjörn Virdung at *ANSYS* for his and their co-operation and involvement, especially for providing the DFM-module.

Trollhättan June 2011

Johan Brunberg and Mikael Aspelin



# Nomenclature

$k$	Thermal conductivity [W/mK]
$Q, q$	Heat flux [W/m <sup>2</sup> ]
$\varepsilon$	Emissivity [-]
$h$	Heat Transfer Coefficient [W/m <sup>2</sup> K]
$G_r$	Grashofs number [-]
$P_r$	Prandtl number [-]
$R_a$	Rayleigh number [-]
$T_{dew}$	Dew-point temperature [K]
$\beta$	Thermal expansion coefficient [1/K]
$\mu$	Dynamic viscosity [kg/ms]
$\alpha$	Absorption coefficient [1/m]
$\rho$	Density [kg/m <sup>3</sup> ]
$\nu$	kinematic viscosity [m <sup>2</sup> /s]
$p$	pressure [kPa]
$g$	gravity [m/s <sup>2</sup> ]
$n$	refractive index [-]
$C_p$	Specific heat capacity [J/kgK]
$\nabla$	Nabla $\left[ \frac{\partial}{\partial x} + \frac{\partial}{\partial y} + \frac{\partial}{\partial z} \right]$
$\Phi$	Scattering phase function
$I(\mathbf{r}, \mathbf{s})$	Radiation intensity, flux per unit normal to ray per unit solid angle
$\sigma$	Stefan-Boltzmann constant $5,6710^{-8}$ [W/m <sup>2</sup> K <sup>4</sup> ]
$\Omega'$	Solid angle
$\sigma_s$	Scattering coefficient
$\mathbf{s}'$	Scattering direction vector

CAD	Computer Aided Design
CAE	Computer Aided Engineering
CFD	Computational Fluid Dynamics
CFL	Courant-Friedrichs-Lewy number [-]
DFM	De-fogging module
LED	Light Emitting Diode
HVAC	Heating, Ventilation and Air-Conditioning
UDF	User-Defined Function
PID	Property Identification
HTC	Heat Transfer Coefficient
RH	Relative Humidity
SAE	Society of Automotive Engineering
OEM	Original Equipment Manufacturer
RTE	Radiation Transfer Equation
DO	Discrete Ordinates
SAAB	Swedish Aeroplane Company limited
URF	Under-Relaxation Factor

# 1 Introduction

In this chapter the background, delimitations, and the methodology used for this project will be found as well as a short description of the physical approach used today.

## 1.1 Background

The automotive world today tends to focus more and more of its resources towards cost effectiveness by incorporating simulations earlier in the development process. This due to increased demands for performance, appearance and new design. New designs of the headlamp involves for instance clear see through casings in which raises new challenges. One of those challenges is condensation that forms on the outer lens which is visualized in Figure 1.1. Since earlier headlamp designs consisted of a dimmer outer lens rather than clear see through, headlamp condensation would now therefore demand more attention from the engineers.



*Figure 1.1 Condensation has taken place on the headlamps outer lens.*

Today, the development process of the headlamp is highly dependent on physical tests, meaning that the construction and geometry of the headlamp has to be revised several times before satisfactory test results can be achieved. This approach is costly and time consuming, by introducing the headlamp to numerical simulations these cost can be reduced. The Figure below shows that the possibilities of making changes to the headlamp decreases with time while the cost of these changes increase with time.

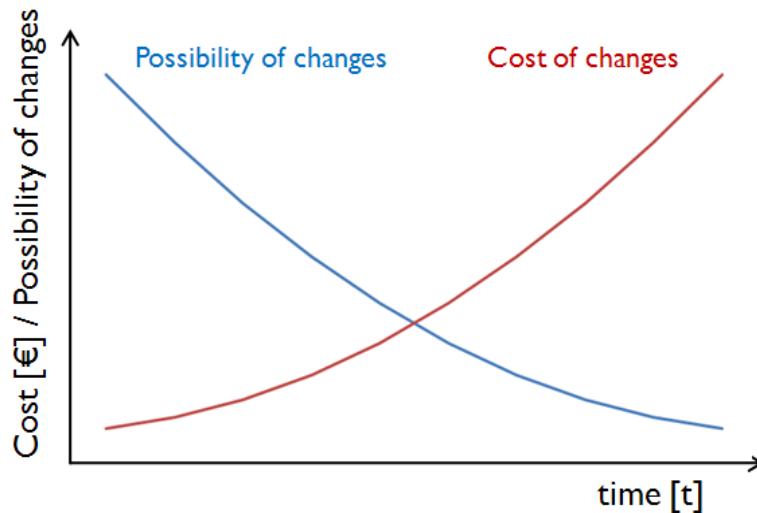


Figure 1.2 Possibility of making changes versus cost of changes in time.

The different costs involve climate tunnel and road tests in order to validate the new headlamp designs.

Condensation is a phenomenon that occurs when the headlamp is submitted to very harsh and moist environments. Since the headlamp is not concealed it will absorb the conditions of the environment as well as those from the engine compartment. These will sometimes lead to fogging of the headlamps outer lens as shown in Figure 1.1.

If the customer finds condensation on the lens, it is opted to fix this and in worst case scenario replace the headlamp. The condensation problem is always evaluated in physical testing and takes a lot of resources to perform as well as unwanted costs. Numerical simulations will therefore be very valuable to the engineers since they will have possibilities to make the necessary changes and improvements on the headlamp early in the design process as well as lowering the costs.

### 1.1.1 Headlamp design

Headlamp performance, appearance, styling characteristics, challenging geometries, functionality, LED and Xenon, energy consumption, transparent see through clear lenses. These are only a few of all the criteria's that needs to be considered while developing a headlamp.

Headlamps are vital for both the performance and the appearance of the automobile. Styling characteristics are demanding more and more challenging geometries and functions for the headlamps, as well as increased demands on function and appearance. Customers and competition on the market demands that the OEM has the latest lightning technology, the headlamp must also remain clean.

The styling trend goes toward LED and xenon lamps that consumes little energy and dissipates much light but little heat. Another styling trend is to use as much transparent materials as possible in the headlamp, which means that the customer can see virtually all internal parts of the headlamp.

The new lightning technology with energy efficient light sources coupled with a lot of transparent materials combined with a harsh and moist environment can sometimes lead to formation of condensation inside the headlamp assembly which can be seen by the customer much easier than early headlamps.

The small amount of heat dissipated from the efficient lamps is not sometimes enough to remove condensation, it will also start some development work at the OEM that will try to find out what is causing the condensation problem. Moisture that will enter the headlamp can also increase wear and corrosion, leading to a shorter lifetime for some components as well as decreasing lightning performance.

The lamp studied in this thesis is a headlamp for a Saab 9-3 which can be observed in Figure 1.3 and 1.4. The headlamp has a high-beam and a low-beam light source. The low-beam consists of the Xenon lamp which can be observed in the middle of the headlamp assembly. To the left is the high beam light source that consists of a Halogen H7 lamp and to the left of the xenon lamp is the light bulb and reflector for the winker light.

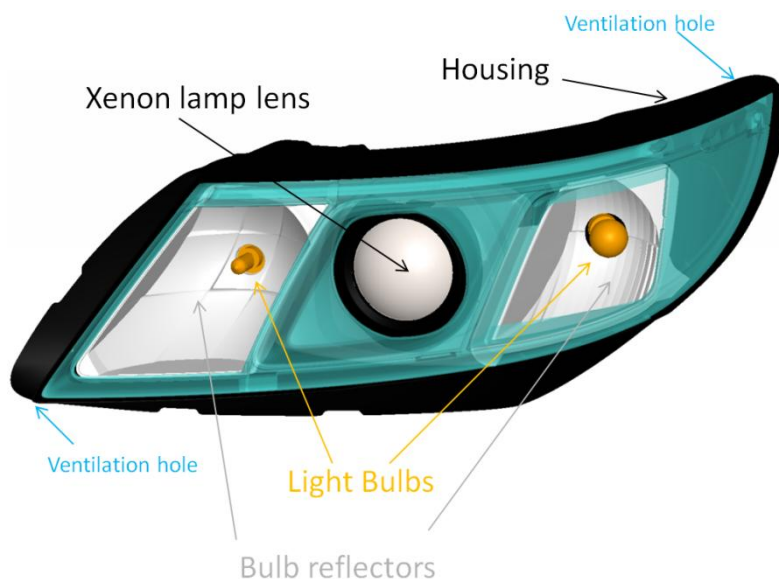
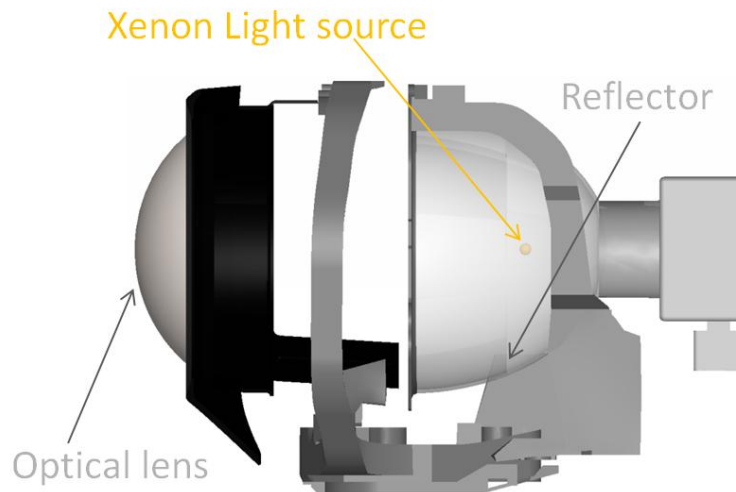


Figure 1.3 Frontal view of the headlamp without the outer lens.



*Figure 1.4 Cross section of the xenon lamp assembly.*

The main light source is the low-beam xenon assembly, which will direct light through the optical lens both via the reflector and focus the light on the road. More about the lamp physics are explained in the theory chapter.

### 1.1.2 Physical approach

Physical testing is performed at Saab in order to test the headlamp and analyze the forming of condensation.

The test used at Saab is performed in their climate tunnel and involves the use of the complete car, which is subjected to a driving cycle with various weather conditions. The Figure below shows a typical climate tunnel test.

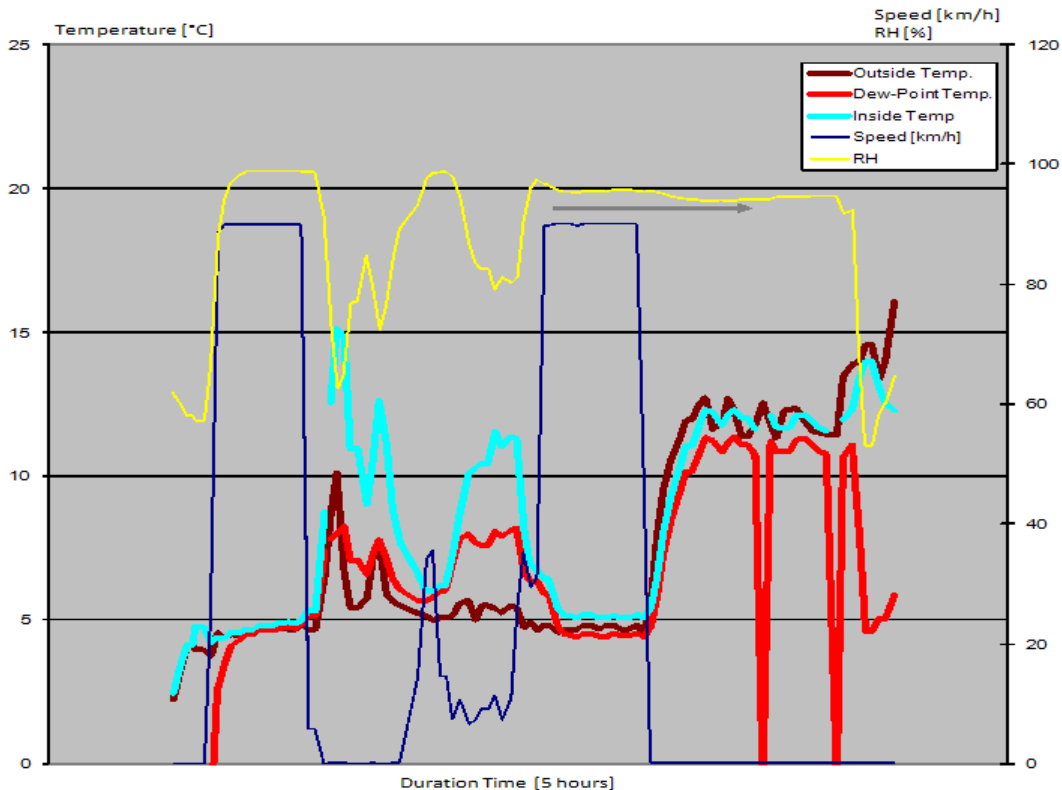


Figure 1.5 Simplified test result obtained from a Condensate-city-cycle test showing temperatures, vehicle speed and environmental parameters.

The part of the test where condensation forms is when the engine runs at idle and cold rain pours down the outside of the lens. The headlamp is thereafter by running the car at high speed for some time. The temperature is measured both outside the headlamp and inside the headlamp, close to the lens. The temperature on the outer side of the lens is measured by using a small sensor, and the inner temperature is measured close to the inner wall of the lens. The relative humidity inside the headlamp is also measured used to calculate the dew point temperature. The total time of the test procedure is about five and a half hours. Condensation is monitored by taking pictures on the outer lens at specific time steps during the test, for instance shown in Figure 1.1.

## 1.2 Objectives

The aim of this study is to develop a numerical method that will predict if and where formation of condensation will occur for the SAAB 9-3 headlamp. Where condensation forms is to be presented visually and should be correlated to previous tests performed in the SAAB Climate tunnel, more specifically the condensation pattern shown in Figure 1.1.

## 1.3 Delimitations

Some delimitations had to be made in order to focus the work on the essentials and to be able to make appropriate simplifications, the delimitations are denoted below:

- Only one headlamp geometry is considered.
- The only heat source is from the low beam xenon lamp
- Necessary simplifications are to be made for the model geometry.
- Boundary conditions will represent one specific point in time.
- Condensation will only be considered on the outer lens.

These limitations were considered from an early stage and supported the development process since it would otherwise have been too many parameters to alter along the way.

## 2 Methodology

In this thesis a numerical method for predicting where condensation forms on the headlamp is going to be developed. This with help of Computational Fluid Dynamics (CFD), the CFD-process consists of three vital steps and are shown and described below.



Figure 2.1 General CFD-process.

### 2.1.1 Pre-processing

The geometry of the headlamp is imported from raw CAD-data. The geometry is then cleaned up depending on the details wanted and the areas of interest. A mesh of triangles are then put on to the surface of the geometry, the size for these triangles can be varied, in this thesis the size of the triangular cells landed between 0.5 to 3mm. The domain is then volume meshed generating a fluid domain in the geometry. Prismatic Layers are then built up in order to take into account solids or to resolve boundary layers. This process was performed in *ANSA*.

### 2.1.2 Solving

The mesh is then exported to the solver where all the physics are set-up and solved. This by applying appropriate boundary conditions for inlets/outlets and walls in the domain along with its specific physical model. The solver solves the mass, momentum and energy equations throughout the domain together with the specified physical model. The equations are discretized along the cells of the domain and solved until convergence is reached. *ANSYS FLUENT* was used as a solver and the calculations were performed on 32 CPU's.

### 2.1.3 Post-processing

The result from the solving is then post-processed. This is where you visualize the results by plotting interesting parameters in different ways. Post-processing was performed in *ANSYS FLUENT*.

### 3 Numerical Simulations

This chapter will show how the numerical method was developed. First by giving an introduction to Heat transfer [7], [8] and fluid dynamics [1] by giving some general theory for each mechanism present in an automotive headlamp then by explaining the governing equations and the physical models used in *FLUENT*.

#### 3.1 Theory

Figure 3.1 below gives an overview of the heat transfer mechanisms that are present in the headlamp and its environment.

The flow of air inside the headlamp depends mainly on natural convection which is forced by the heat from the light bulb. The light bulb will heat the surrounding air and force the hot air to rise as new colder air enters from below. Radiation from the sun and the light source will be reflected by the reflector and energy will be absorbed by the nearby surfaces and cause the adjacent air to be heated. The heat absorbed by the surfaces will be transported through the materials by heat conduction.

The headlamp casing is equipped with two ventilation holes that allows the headlamp to breathe. The ventilation holes are also the only way for moisture to enter and exit the domain. Each mechanism will be described further in the subchapters below.

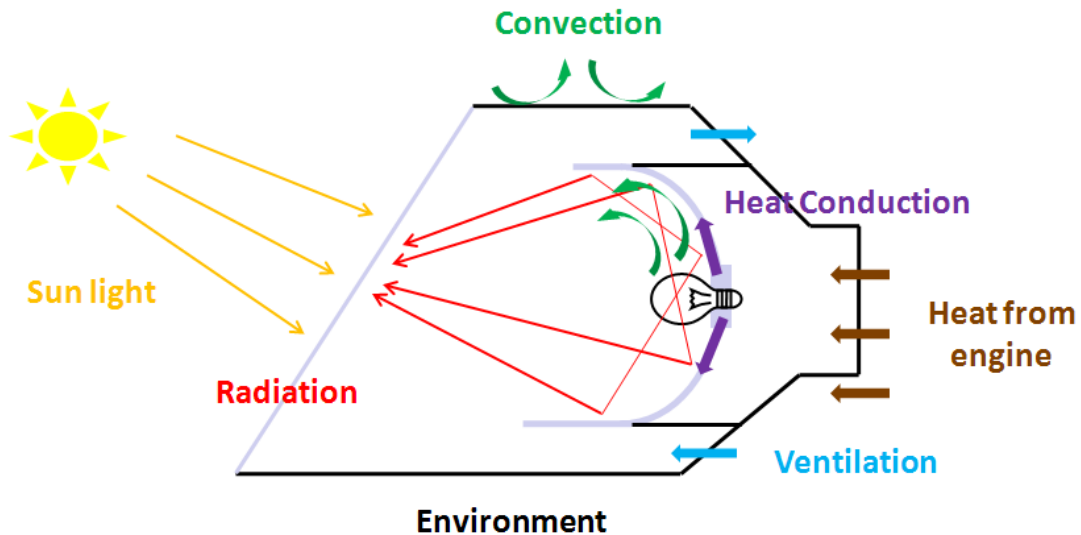


Figure 3.1 Heat transfer mechanism on the lamp.

### 3.1.1 Convection

Natural convection is usually recognized as movement of air induced by temperature changes, and is also known as buoyancy driven flow. As the temperature of the fluid rises, the density will decrease, thus the warmed air will start to move upward, being replaced by colder air moving in from below. Buoyancy driven flows are characterized by constants like the Grashof number which is used to describe the ratio between the viscous forces and the buoyancy forces. The intensity of natural convection can be measured by the magnitude of the Rayleigh number.

The Rayleigh number indicates the difference between viscous and buoyancy forces in the fluid and a large value implies strong natural convection effects. The Prandtl number describes the ratio between the fluids kinematic viscosity and thermal diffusivity.

$$G_r = \frac{\beta \cdot g \cdot L^3 \cdot \rho^2 \cdot \Delta T}{\mu^2} \quad (3.1)$$

$$R_a = G_r \cdot P_r = \frac{\beta \cdot g \cdot L^3 \cdot \Delta T}{\nu \cdot \alpha} \quad (3.2)$$

Where  $\beta$  is the thermal expansion coefficient,  $g$  is the gravitational constant,  $L$  is the characteristic length,  $\rho$  is the density of the fluid,  $\nu$  is the kinematic viscosity [ $\text{m}^2/\text{s}$ ],  $\alpha$  is the thermal diffusivity [ $\text{m}^2/\text{s}$ ],  $\Delta T$  is the temperature difference between the surface and the fluid and  $\mu$  is the dynamic viscosity.

The critical Rayleigh number where transition to turbulence occurs is between  $10^8$  and  $10^9$ , values above this indicate turbulent flow.

Convection is the mechanism where heat is transferred between a solid material and the fluid around it as the fluid flows against the surface of the solid. Convection is a mixture of conduction and the motion of a fluid and as the fluid motion increases, so does the convective heat transfer.

When the fluid is in motion, heat is transferred by convection, and when the fluid motion is infinite, heat is transferred by conduction.

$$\dot{Q}_{convection} = h \cdot A \cdot (T_s - T_\infty) \quad (3.3)$$

Where  $h$  = Heat transfer coefficient [ $\text{W}/\text{m}^2\text{°C}$ ],  $A$  = surface area [ $\text{m}^2$ ],  $T_s$  = surface temperature [ $\text{°C}$ ] and  $T_\infty$  = free stream temperature of the fluid [ $\text{°C}$ ].

HTC depends on the surface geometry, the flow field around the surface as well as the fluid properties and velocity.

### 3.1.2 Conduction

When two regions have a temperature difference, energy is transferred between the two by conduction. Conduction usually takes place in or between interaction surfaces and solids. The heat transport occurs spontaneously from the warmer medium to the cooler due to the temperature gradient between the two.

The two regions strive for equilibrium, thus conductive heat transfer will stop when the temperature difference between the two mediums are zero. Heat that is being transferred through a medium by conduction can be expressed by Fourier's law.

$$\dot{q}_x = -k \cdot \frac{\Delta T}{\Delta x} \quad (3.4)$$

Where  $k$  = thermal conductivity coefficient [W/m°C],  $\Delta x$  = wall thickness [m],  $\Delta T$  = temperature difference between the mediums [°C].

Thermal conductivity is a material specific property that defines how much heat that can be transported through the material. Thermal conductivity varies with material temperature. A high thermal  $k$ -value indicates good thermal conductivity, meaning that the material conducts more heat.

### 3.1.3 Radiation

The energy emitted by an energy source is described as radiation of electromagnetic waves. These waves do not need any medium to be transferred and radiation is therefore fastest in vacuum where nothing restricts the electromagnetic waves.

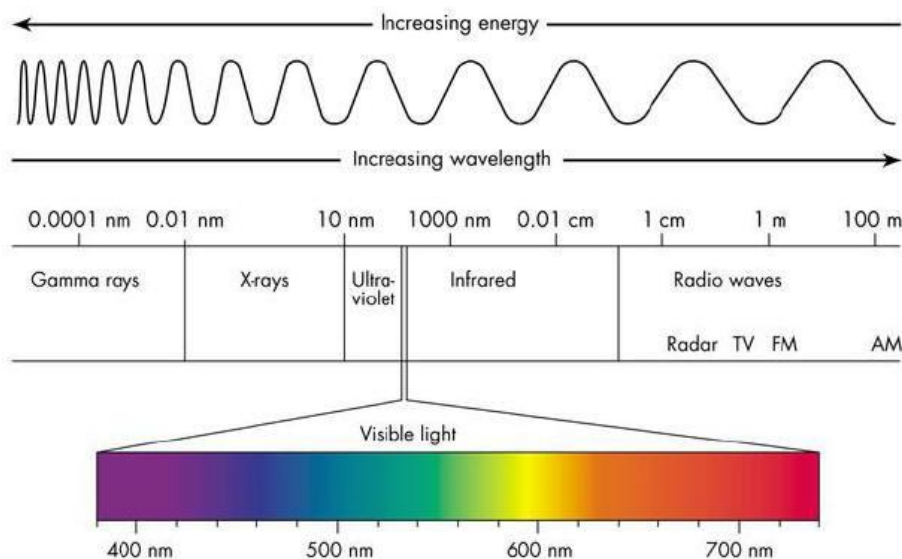


Figure 3.2 Electromagnetic wave spectrums.

Electromagnetic waves are spread over a wide spectrum of wavelengths where each part of the spectrum has vast differences in their properties compared to other parts of the spectrum. Over the electromagnetic wave spectrum Figure 2.3, thermal radiation only includes wavelengths between 0,1 and 100 [ $\mu\text{m}$ ], and visible light is in the range between 0,4 and 0,76 [ $\mu\text{m}$ ]. Thermal radiation is emitted by all bodies with a temperature above absolute zero, i.e. above zero degrees Kelvin. The amount of radiation emitted from a body can be expressed by Stefan-Boltzmann law below.

$$\dot{Q}_{radiation} = \varepsilon \cdot \sigma \cdot A \cdot (T_s^4 - T_\infty^4) \quad (3.5)$$

Where  $\varepsilon$  = Emissivity [-],  $T_s$  = surface temperature [K],  $T_\infty$  = surrounding temperature [K],  $A$  = surface area [ $\text{m}^2$ ] and  $\sigma = 5,67 \times 10^{-8}$  [ $\text{W}/\text{m}^2 \times \text{K}^4$ ].

Emissivity is a material property and the emissivity of a surface is equal to one for a black body and close to zero for a highly reflective material. The shiny surface of a reflector has an emissivity value between 0,05 to 0,1, while dark colored surfaces have values up to 0,98. Emissivity depends on wavelength, surface temperature and the incoming radiation angle. A surface can emit, transmit or absorb radiation, the absorption  $\alpha$ , which is the amount of radiation that is being absorbed by a surface. A body that absorbs all incoming light has an absorption coefficient of one. Absorbing radiation will cause the body temperature to increase. Both the emissivity  $\varepsilon$  and absorption  $\alpha$  depends on the surface temperature and the wavelength of the incoming radiation. These values can on the other hand be estimated as an average if the surrounding radiation is of the same order of magnitude as the surface temperature, which often is the case. The values of  $\varepsilon$  and  $\alpha$  are often estimated as constant values for all temperatures and wavelengths, and is called gray body radiation. Transmissivity means that a large amount of the incoming radiation is being transmitted through the material, if the material transmits radiation in the visible range, it is optically transparent. If no transmission of radiation in the visible range occurs, the material is opaque. Light that is being transmitted through a material can also be scattered, scattering mainly depends on impurities or structural disorder and could be seen as a measure of particles and irregularities in the structure of the material scatter and reflect the light, prohibiting some of the light to be transmitted.

### 3.1.4 Condensation

The air mainly consists of five substances; nitrogen, oxygen, argon, carbon dioxide and water vapour. The amount of water vapour that can be obtained by air can be expressed as the relative humidity (RH) and is limited by the temperature and pressure of the air, thus the maximum relative humidity varies with two parameters. If the pressure drops or the temperature rises when  $RH=100\%$ , water will deposit from the air and form dew. If air with a relative humidity of 100% gets in contact with a cold object with a surface temperature below the current dew point, water will deposit from the air onto the surface of the object.

The dew point temperature is the critical temperature at a certain pressure for which the air cannot withhold more water vapour. The dew point temperature can be defined as *“the temperature to which the air would have to cool at, constant pressure and vapour content, in order to reach saturation”* according to [15]. The dew point temperature can never be higher than the air temperature, thus water vapour is removed from the air with the condensation mechanism when the temperature drops below the dew point.

Condensation is formed as small water droplets and can be seen as fog (as often seen in valleys or at sea after sunrise) or as small droplets on the surface of cold objects such as glass windows or cold soda cans.

The condensations phenomena inside an automotive headlamp can simply be explained by the inner surface of the transparent lens having a temperature equal to or above the current dew point of the air adjacent to the lens. This usually occurs locally around the lower edge of the lens and slowly grows upwards depending on how severe the circumstances are. Most analysis on the subject simplifies the condensation on the inside of the lens as film condensation and so will also be the case in this thesis work. It is also considered conservative to assume film condensation according to [1].

For condensation to be able to occur, the moist air has to come into contact with a cold surface. The coldest surface in the headlamp is usually some areas on the outer lens which offers poor insulation against the environment, heat is also more easily dissipated through the transparent material. The lens therefore gets cooled quickly and provides the heat transport necessary to cool the lens and adjacent air below the dew temperature. Energy is also being released from the water vapour when it cools to liquid and that energy is quickly transported away through the lens. Some areas of the lens are however warmed by radiation from the lamp and by the flow of air that has been warmed by the lamp. The temperature variations on the lens result in a certain pattern where condensation is more likely to form.

The relative humidity or dew point of the air can be specified with the help of a Mollier or psychometric chart, as seen in Figure 2.2 below where a simplified Mollier chart is presented. The curved blue line at the right represents 100% relative humidity and at a given pressure, the saturation temperature of the water vapour can be read.

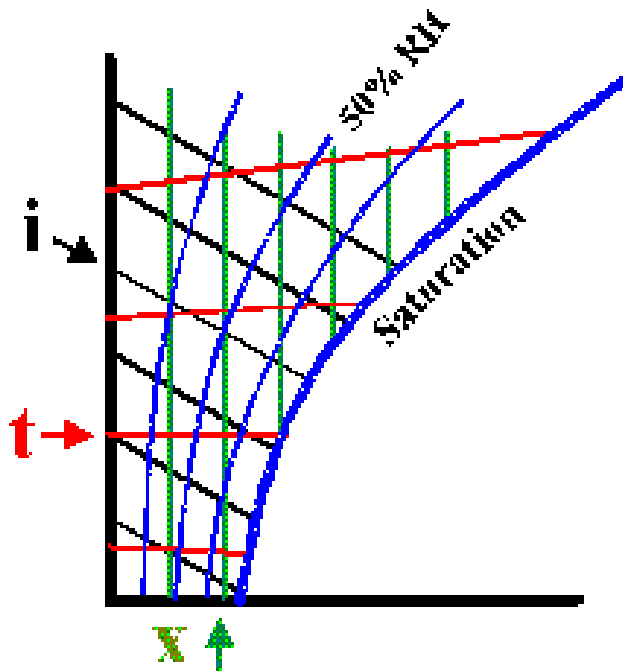


Figure 3.3 Simplified Mollier chart.

Where

$i$  = Enthalpy [Joule],  $t$  = Temperature [ $^{\circ}\text{C}$ ],  $x$  = Water vapour content of air [kg/kg],  
 RH = Relative humidity [%]

Another way to determine the dew point is by using the Magnus Tetens formula [3] which was included in the work by Bahrenburg [19].

$$T_{dew} = \frac{b \cdot \alpha(T, RH)}{a - \alpha(T, RH)} \quad (3.6)$$

And

$$\alpha(T, RH) = \frac{a \cdot T}{b + T} + \ln(RH) \quad (3.7)$$

$$a = 17,27$$

$$b = 237,7^{\circ}\text{C}$$

$T$  = Temperature in  $^{\circ}\text{C}$ , RH = Relative Humidity,  $T_{dew}$  = Dew Point Temperature.

The equation is only valid for a relative humidity between 1 and 100%, i.e.  $RH = 0.01$  and 1.0. It is also only valid for air temperatures between  $0^{\circ}\text{C}$  and  $60^{\circ}\text{C}$ , as well as dew point temperatures between  $0^{\circ}\text{C}$  and  $50^{\circ}\text{C}$ . Since the formula is based on some approximations the resulting dew point temperature will have an uncertainty of about

$\pm 0,4^{\circ}\text{C}$ . If the temperature of the air and water vapour mixture is close or equal to the calculated dew point temperature, there is a high possibility for condensation to form.

Condensation is a phenomenon which occurs when the vapour is cooled below its saturation temperature. In this case with condensation inside the headlamp, mainly film condensation will occur. Film Condensation occurs when the temperature of the wall adjacent to the water vapour cools below the saturation temperature, in which the adjacent vapour will also cool below the saturation temperature and form condensation on the wall. Heat is then transferred from the film layer to the wall, keeping the condensation film below the saturation temperature. This mechanism increases heat transfer drastically and according to [2], condensation can increase the heat transfer by as much as 100 times compared with an air-wall situation.

### 3.1.5 Fluid dynamics

The fundamental and governing equations regarding fluid flow and heat transfer are the conservation of mass (continuity equation), conservation of momentum (Newton's second law) and the energy equation. These can be further studied in [1].

Conservation of mass states that the amount of mass that enters a system must be equal to the amount that leaves the system.

$$\nabla \mathbf{u} = 0 \quad (3.8)$$

Where  $\mathbf{u}$  is the velocity vector.

Conservation on linear momentum (Newton's second law) for a Newtonian fluid keeps a relation between the pressure, momentum and viscous forces.

$$\rho \frac{\partial \mathbf{u}}{\partial t} = -\nabla p + \mu \nabla^2 \mathbf{u} + \rho \mathbf{g} \quad (3.9)$$

Where

$\rho$ =density,  $p$ =pressure,  $\mu$ =viscosity,  $g$ =gravity field

The Energy equation states the total amount of energy is conserved in the system.

$$\rho \frac{\partial T}{\partial t} C_p = k \nabla^2 T + \Phi \quad (3.10)$$

Where

$C_p$ =ratio of specific heat,  $T$ =temperature,  $k$ =thermal conductivity  $\Phi$ =function for viscous dissipation

## 3.2 Numerical Setup

As stated in Chapter 1, condensation will only form at specified walls and the mesh for that wall has to be built up in a very specific way. The mesh was built up considering these requirements. In able to use the DFM-module some aspects had to be considered when developing the mesh. [9], [10], [11] and [12].

In order to keep both cell skewness and aspect ratio within the requirements one has to decrease the cell size, but this will cause aspect ratio to go up due to the physical thickness of the lens.

### 3.2.1 Computational grid

The headlamp geometry is very complex as seen in Figure 3.1 and when importing the CAD into ANSA information is lost on the way and has to be fixed before the meshing process. This resulted in a long CAD-cleaning process.

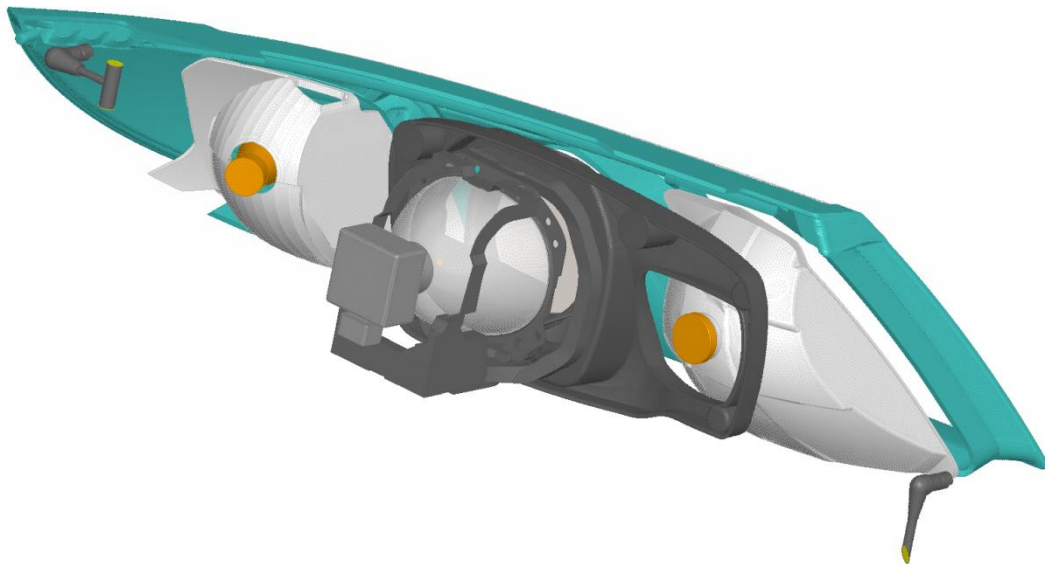


*Figure 3.4 Headlamp mesh.*

*A=Winker reflector, B=Xenon lamp reflector, C=Xenon lamp frame, D=Xenon lamp frame holder, E=Halogen high beam reflector, F=Main frame/carrier.*

Areas where surfaces were complex consisting of narrow gaps, small angles, tight compartments etc. had to be simplified.

The low beam light source in the xenon lamp stood for the most complex geometry of the headlamp. Therefore the geometry had to be simplified and it was chosen to remove the bulb and only keep the filament that is the actual heat source.

The filament was reduced to a small single sphere with a diameter of 3 millimetres, suspended freely in the air. The assumption was that the light bulb geometry itself had little effect on the flow of air inside the lamp and didn't affect the airflow at the lens. The xenon lamp mesh is depicted below:

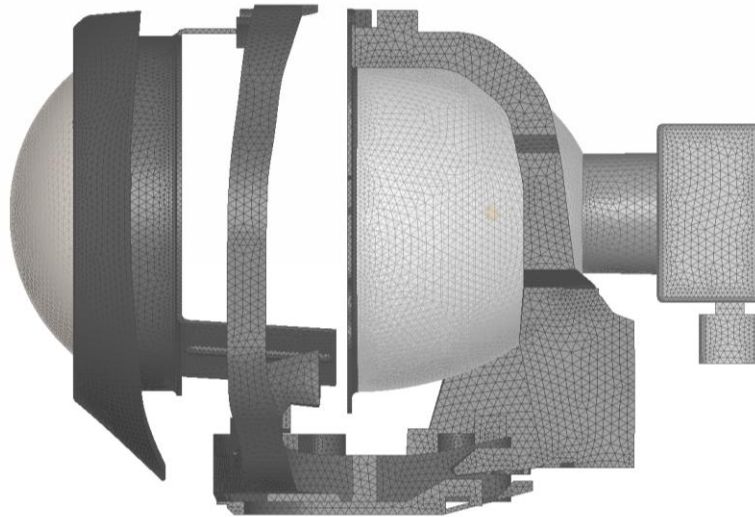


*Figure 3.5 Xenon lamp mesh.*

*A=Xenon lamp filament. B=Xenon light bulb casing. C=Xenon lamp transistor box. D=Xenon lamp reflector plate. E=Xenon lamp frame. F=Xenon lamp lens glass. G=Xenon lamp lens holder frame.*

Some inner parts of the headlamp are very thin and were therefore not volume meshed as solids, in order to gain from such choice the solver will require a lot of nodes through the thickness in order to obtain an adequate solution. This would require the cell size to be very low and therefore thin inner parts with a thickness of 1 millimetres or less was chosen to be surface meshed as ordinary zero-thickness walls. Thicker parts could be meshed as solids but also chosen not to. The final mesh is depicted below:

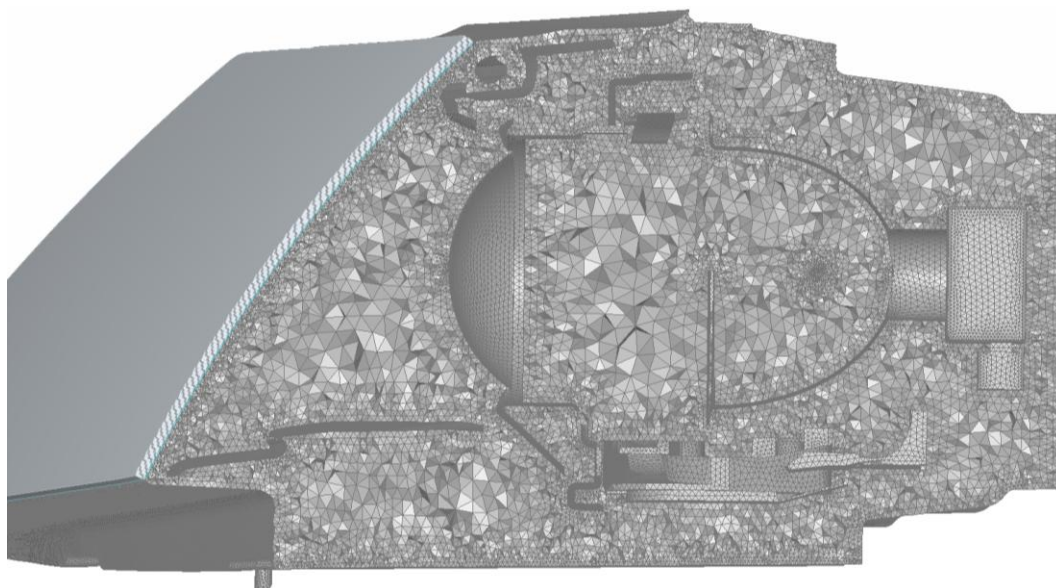


*Figure 3.6 Cross section showing the headlamp volume mesh.*

The outer lens was chosen as the only part where condensation is to be formed. Prismatic layers were therefore extruded on top of the outer lens. The first layer extruded should represent the area where moist air is at saturation temperature. It was chosen to only model 2 layers since the actual film thickness is expected to be very thin and that the boundary layer doesn't require  $y^+$  estimation since turbulent flow isn't attending.

The outer lens is then extruded on top of this layer, consisting of 5 prismatic layers with a total thickness of 2.6 millimetres, thus positioning the outer lens some distance away from its original position.

This type of design generates the wall on which condensation is to be formed, the wall generated between these layers will consist of two-sides, which are connected to the DFM. The layers are depicted in the Figure below:

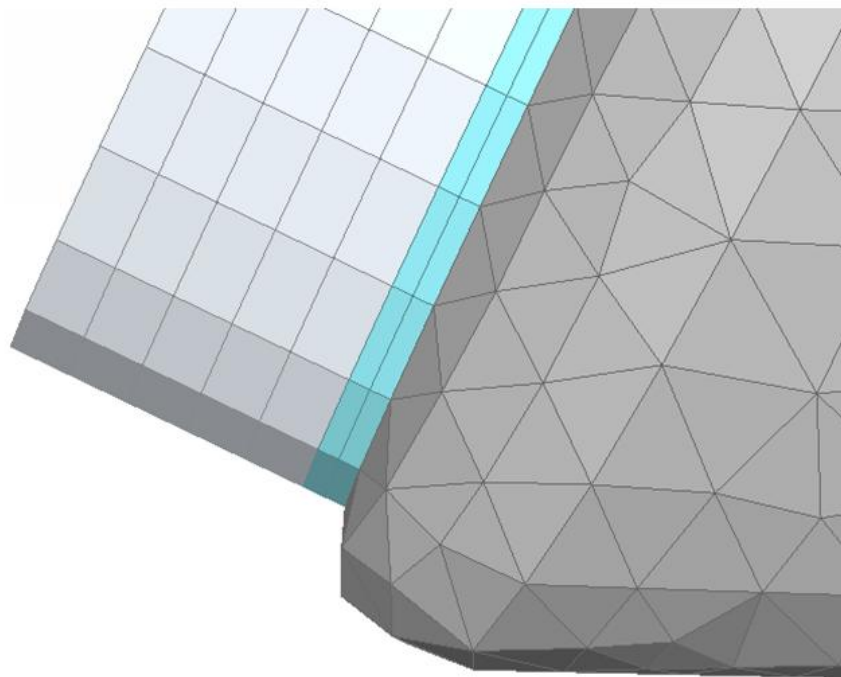


*Figure 3.7 Close-up view of the prismatic layers representing Thickness of the outer lens (light gray) and layers on which condensation will form (light blue).*

Table 3.1 Shows the final cell size and total amount of cells for the computational domain

	[mm]	[million]	Quality
<b>Cells</b>			
Surface	0.5-3.0	1.1	
Volume	0.5-8.56	10.8	
<b>Prism layers</b>			
Outer lens	5·0.567	1.0	
Moist-air	2·0.2	0.3	
<b>Quality</b>			
Cell skewness			0.946
Aspect ratio			0.289
Cell squish			0.780

### 3.2.1.1 Convection

There are two methods to model natural convection in *FLUENT*, one is to use the Boussinesq approach and the other one is to use the Incompressible ideal gas approach [4] and [5]. According to the guidelines in [4] and [5] the Boussinesq approach is not recommended to use if the temperature variations in the domain are large. Since it was approximated that the filament temperature will be set as a constant temperature of 2000°C and the outside temperature is 5°C it is very likely that the temperature variations in the domain will be large. Therefore it was determined to use the Incompressible ideal gas approach.

To use the Incompressible ideal gas approach, guidelines from *FLUENT* Users Guide [4] and [5] was used specifying following:

Density of air: Incompressible-ideal-gas

Specified Operating density: 1.225 kg/m<sup>3</sup>

Energy: On

Gravitational acceleration: 9.81 m/s<sup>2</sup>

Operating pressure: 101325 Pa

The numerical schemes used for solving buoyancy driven flows are either the Body Force Weighted or PRESTO, and Body Force Weighted was chosen according to guidelines [4] and [5].

Modelling of Convective heat transfer is done by specifying the HTC in the mixed thermal conditions tab in the boundary conditions panel. Since radiation will be present one can also specify both the external and internal emissivities and external temperatures.

The HTC is specified on the outer surfaces describing the heat transfer from the surrounding environment.

### 3.2.1.2 Conduction

Modelling heat conduction in *FLUENT* can be done in several ways according to [4] and [5]. The thermal conductivity of the material is used for the calculation of thin-wall thermal resistance and specified in the thermal conditions panel. Material properties and thickness are specified.

When specifying a thickness for a wall with zero-thickness *FLUENT* will create a virtual layer from that wall and calculate heat transfer in the 1D direction. Heat conduction can also be considered in the planar direction by using the Shell conduction approach. One disadvantage with the shell conduction model is that it can't be used for semi-transparent walls.

The Materials and the properties used are specified in Appendix A.

### 3.2.1.3 Radiation

Five different radiation models are available in *FLUENT* but only one of them can solve problems involving semi-transparent walls. It is called the Discrete Ordinates (DO) model. Radiation is solved in *FLUENT* by using The Radiation Transfer Equation (RTE) [4] and [5].

The RTE is based on this following formula:

$$\underbrace{\nabla[I(\mathbf{r}, \mathbf{s})\mathbf{s}] + (a + \sigma_s)I(\mathbf{r}, \mathbf{s})}_{\text{Absorption}} = \underbrace{an^2 \frac{\sigma T^4}{\pi}}_{\text{Emission}} + \underbrace{\frac{\sigma_s}{4\pi} \int_0^{4\pi} I(\mathbf{r}, \mathbf{s}')\phi(\mathbf{s}\mathbf{s}')d\Omega'}_{\text{Scattering}} \quad (3.11)$$

Where

$I(\mathbf{r}, \mathbf{s})$  = Radiation intensity, flux per unit normal to ray per unit solid angle or direction

$a$  = Absorption coefficient

$\sigma_s$  = Scattering coefficient

$\mathbf{s}'$  = scattering direction vector

$\sigma$  = Stefan-Boltzmann constant

$\Phi$  = Scattering phase function, probability that a ray from one direction will be scattered into the same direction as another ray

$n$  = Refractive index

$\Omega'$  = solid angle

The DO model uses a discretization technique which solves the RTE for a finite number of angles or directions [5]. The angular discretization is controlled by either increasing or decreasing the amount of theta-phi divisions and pixels [5]. The number of divisions and pixels should therefore be kept at a minimum in order to keep computational cost as low as possible, but the minimum amount will also give the coarsest discretization.

The settings vary between a minimum of 1x1x1x1x which is the coarsest to 10x10x10x10 which is the maximum and gives the highest accuracy and finest discretization. Since maximum discretization costs a lot of computational time and data storage the angular discretization used in the radiation model was determined to 3x3x3x3 which would be sufficient.

Semi-transparent walls will depend on the material properties specified and the transmitted radiation that will exit the domain, the effect of solar radiation can be specified but was not chosen for this case. The diffuse fraction can be set, indicating if the incoming radiation is to be reflected for a rough or mirror-like surface. This can be specified by changing the diffusive fraction value in the radiation boundary conditions panel between 0 and 1.

### 3.2.1.4 De-Fogging Module (DFM)

The DFM was at first developed for de-fogging and de-icing simulations for HVAC applications. But since the physics behind it are the same as for the condensation phenomena it could be used for predicting condensation.

The DFM is written as a User-defined Function (UDF) and provided by ANSYS. The DFM is still under development and was used to evaluate how well it could perform for headlamp condensation problems.

The tutorial for the DFM provided by ANSYS has been used to specify each boundary condition. Each boundary conditions are coupled to the DFM in which will solve Fick's first law of diffusion which relates the diffusive flux that goes from regions of high concentration to regions of low concentration [4] and [5], this is handled in FLUENT by Species transport and the energy equation. Equations that are stated below:

Energy equation with species diffusion according to [4] and [5] as follows:

$$\frac{\partial(\rho E)}{\partial t} + \nabla[\vec{V}(\rho E + p)] = \nabla \left[ k \nabla T - \sum_j h_j J_j \right] + S_h \quad (3.12)$$

Energy per units mass:

$$E = h - \frac{p}{\rho} + \frac{V^2}{2} \quad (3.13)$$

The energy source due to species diffusion is included through this term:

$$\nabla \left( \sum_j h_j J_j \right) \quad (3.14)$$

And will include the effect of enthalpy transport due to species diffusion.

$$J_i = -\rho D_{i,m} \nabla Y_i - D_{T,i} \frac{\nabla T}{T} \quad (3.15)$$

Where

$J_i$  = Diffusion flux of species i [mol/m<sup>2</sup>s]

$D_{i,m}$  = Mass diffusion coefficient for species i [m<sup>2</sup>/s]

$D_{T,i}$  = Thermal diffusion coefficient [mol/m<sup>3</sup>]

Some assumptions and simplifications are made in the DFM and stated below:

1. Condensation will only occur at specified surfaces.
2. The condensation film is fully contained by the first layer of cells adjacent to the specified walls.
3. Condensation mass transfer rates are determined only by the gradient of water vapour mass fraction in the cells containing the condensation film.
4. The condensation film is stationary
5. The inlet relative humidity is constant in time
6. Gravity and surface tension effects of the condensation film is neglected
7. The Diffusion coefficient of water vapour in moist air is known as a function of local pressure and temperature, Mollier chart or the Bahrenburg approach [18].
8. Inlet and outlet mass flow rates of water vapour is much higher than the mass transfer through condensation

The relative humidity at the inlets and domain was then specified to match the conditions at the experimental test in the Climate tunnel at one specific time step. The inlet and domain relative humidity was set to be 90%. The initial film thickness was zero millimetres.

### 3.2.2 Solution Process

In order to obtain a solution for the condensation problem a solution algorithm was developed. Once the mesh was finalized it was exported to *FLUENT* for the numerical setup, the solution algorithm are depicted in the Figure below:

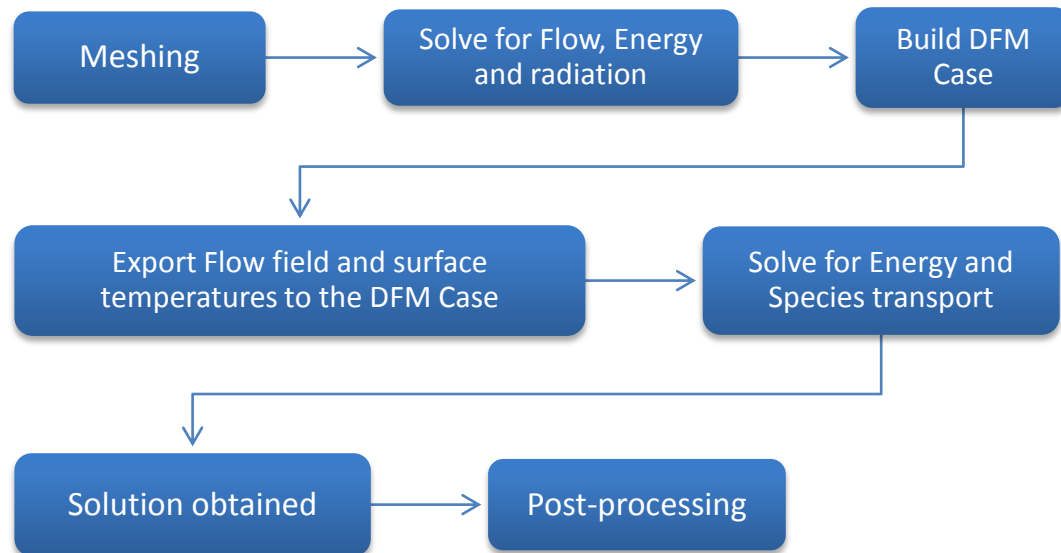


Figure 3.8 Chart describing the solution process from start to finish.

At the beginning two cases are built parallel. One case that will handle buoyancy driven flow, convection, conduction and radiation. The second case to handle condensation.

For case one the boundary conditions stated earlier was used. In order to obtain a steady state solution, the numerical scheme used was SIMPLE for pressure-velocity coupling. Body force weighted for pressure.

The case was then run with first order discretization for 1000 iterations, then switched to second order discretization for 2000 more iterations. Monitoring was made for interesting surfaces in order to follow the temperature, velocity residuals. If the residuals didn't change more than  $1e-6$ , or the temperature was nearly constant for an adequate number of iterations one could say that the solution was converged [4].

Case two was built by specifying boundary conditions for the DFM for the same mesh as case one. Most important is the wall on which condensation is to form, as mentioned before the wall is two-sided and require both sides to be solved from the DFM.

The pressure, temperature and velocity field are then saved into interpolate files and imported into case two.

The numerical algorithm is changed from SIMPLE to PISO with standard settings. Equations activated for the transient solving are to be Energy and H<sub>2</sub>O for Species transport. URF for Energy and H<sub>2</sub>O is maintained between 0.95-1.0. Case two was then run for 1 time step of 0.1 seconds and was converged after 38 iterations.

Investigation of the CFL number will then state if the solution is valid and should in this case be in the range of 20-40.

## 4 Results

In order to evaluate the results, important parameters such as the temperature distribution, velocity distribution and condensation film thickness was plotted in different point of views. Comparisons have also been made by comparing the plots from numerical simulations versus climate tunnel testing and photos taken from an infrared camera.

### 4.1 Temperature distribution

Figure 4.1-4.2 below shows the temperature distribution on the outer lens, both taken from simulations and infrared camera. When the photos was taken with the infrared camera, the ambient conditions such as outside temperature, relative humidity and radiation was not the same as the ones used in the simulation, therefore one can only compare the pattern of the temperature distribution, not the temperature magnitude.

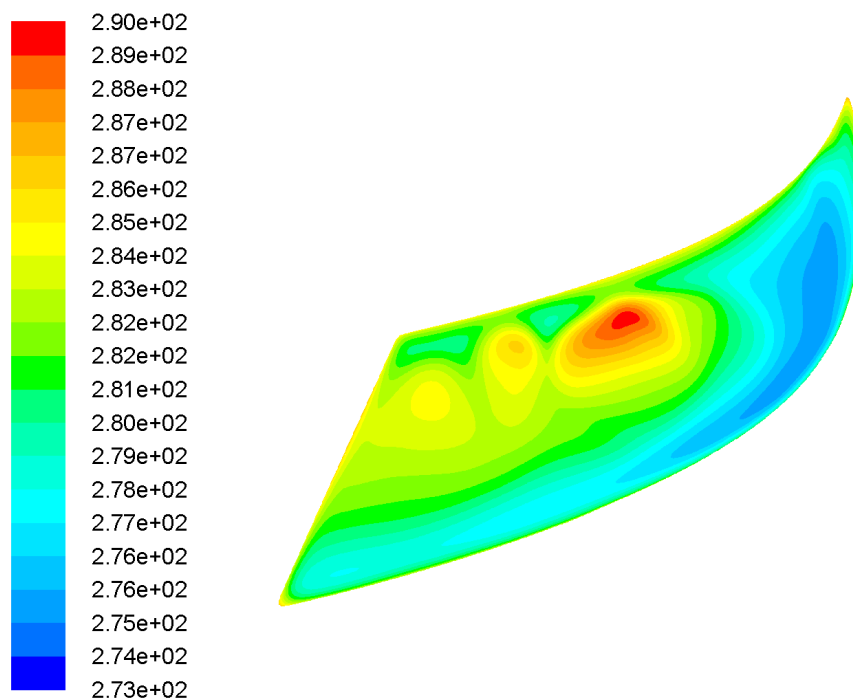


Figure 4.1. Temperature distribution [K] on the outer lens taken from simulation ambient temperature = 278K.

One can also see that a match is confirmed when comparing the temperature pattern from the simulation and infrared camera when the low beam is OFF, Figure 4.2. But when comparing with the light beam ON one can notice a deviation. A possible explanation for this is that the radiation model somehow does not transfer the light through the optical lens correctly.

When the headlamp is turned on the xenon lamp will heat up the outer lens by radiation and focus the light on the road. Focusing of the light occurs through the optical lens and can be seen in figure 4.2a. One can also notice an additional pattern on the outer lens, which is the focused light. This pattern will disappear as soon as the headlamp is turned off and what we have left is only the conductive part, figure 4.2b. By comparing these patterns with the simulation it is clear that the result reassembles figure 4.2b. This means that the simulation model does not capture the effect of radiation fully and only captures the conductive part.

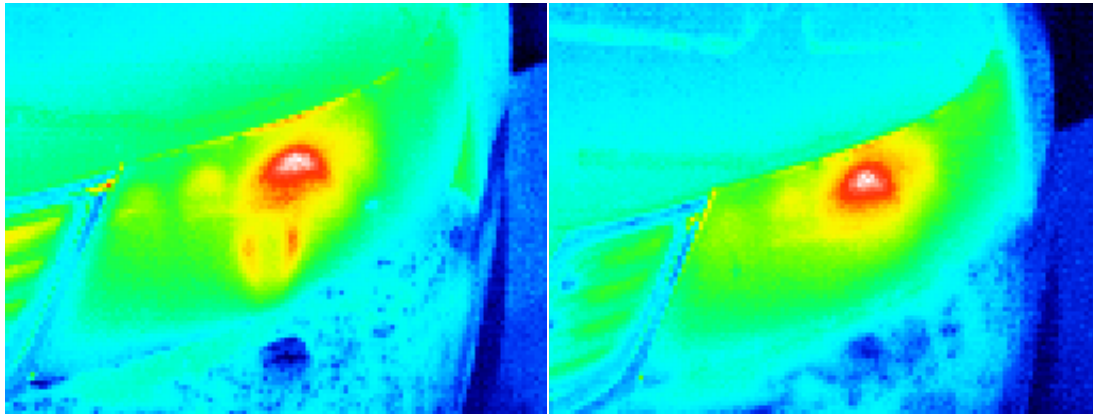


Figure 4.2. Temperature distribution measured with IR Camera.

a) light beam ON.      b) light beam OFF.

The temperature distribution was also plotted from a cross-section point of view from the xenon-lamp in order to view the in-depth distribution. In the Figure below one can see that the temperature are highest surrounding the xenon light source. Heat will rise and warm the adjacent surfaces. One can also see that areas far from the light source and not in the direct path with radiation will be of a lower magnitude of temperature. It is these areas that are most prone for condensation to occur.

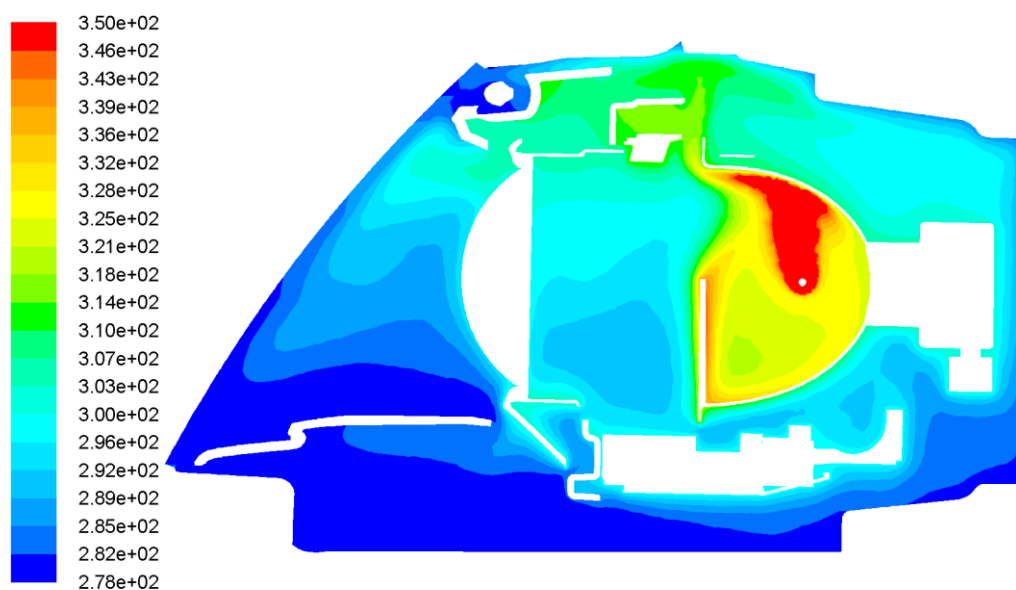


Figure 4.3. Cross section through the xenon lamp showing temperatures [K].

## 4.2 Velocity distribution

The velocity distribution is of high importance since the headlamp is an open system that regards both the in- and outflow of warm and cold moist air. It is essential to have a perfectly balanced in- and outflow system that evacuates unwanted moist air so it doesn't get stuck on the outer lens or builds up as water deposits. The Figure below shows velocity vectors colored by temperature at the headlamps outer lens. In this plot one can see that there are regions where there are both high velocities with low temperature amongst with regions of low velocities with high temperatures. These regions are magnified and can further be studied in Figures 4.5-4-6.

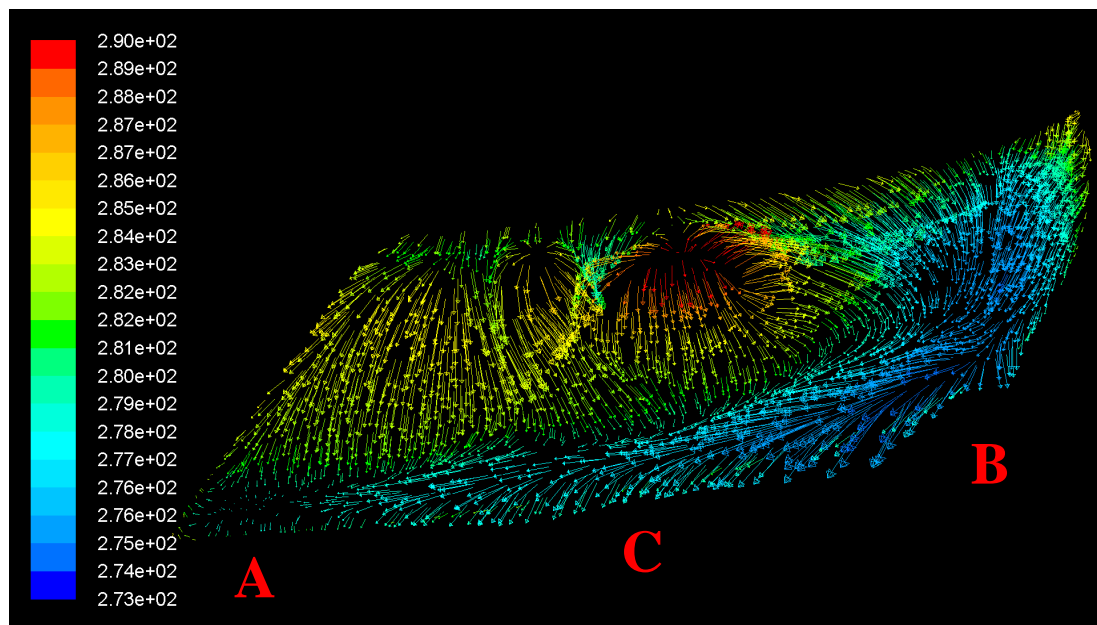


Figure 4.4 Velocity vectors colored by temperature on the outer lens.

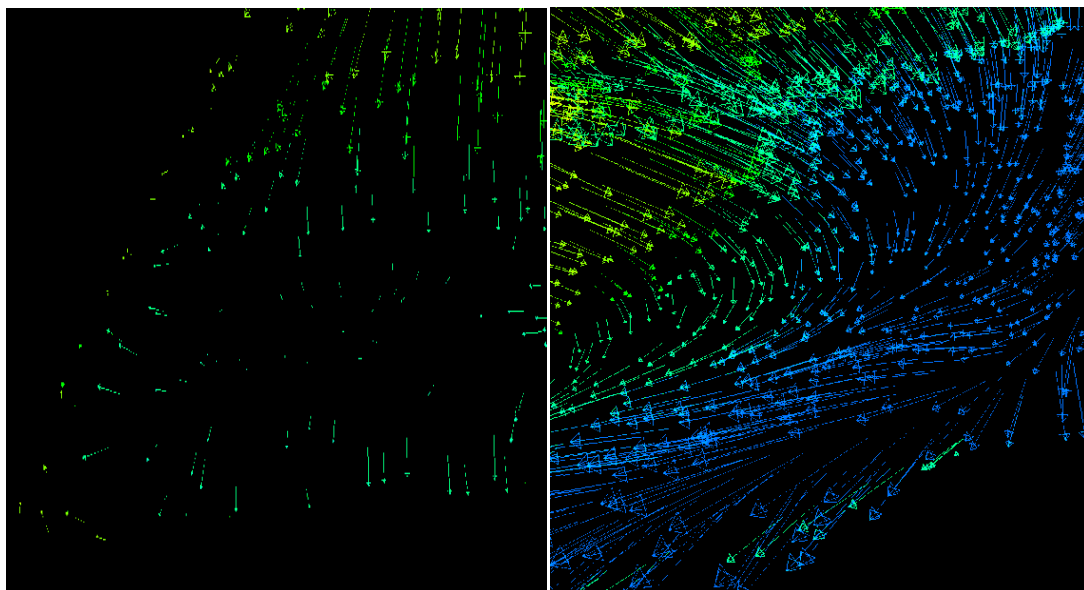
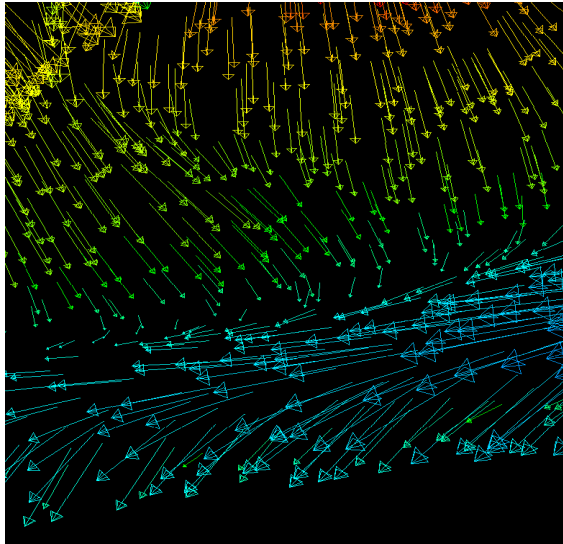


Figure 4.5 Region A & B, High temperature with low velocity and high velocity with low temperature.

The moist air that region A contains has difficulties to be evacuated and replaced with new fresh air due to the low velocity in that area. The opposite occurs at region B where instead the velocity is high but the cold moist air remains cold and moist.

Region C in Figure 4.6 below indicates medium velocity that decreases as it approaches region A. Investigating this further by comparing with temperature and condensation distribution pattern from the physical testing shows that there is a deviation in region C. This confirms earlier statements in chapter 4.1.



*Figure 4.6 Region C, middle region.*

### 4.3 Film thickness

The transient simulation enabled forming of condensation on the outer lens, and the result can be seen in the Figure below. The Figure shows the film thickness of condensation that has formed at the outer lens.

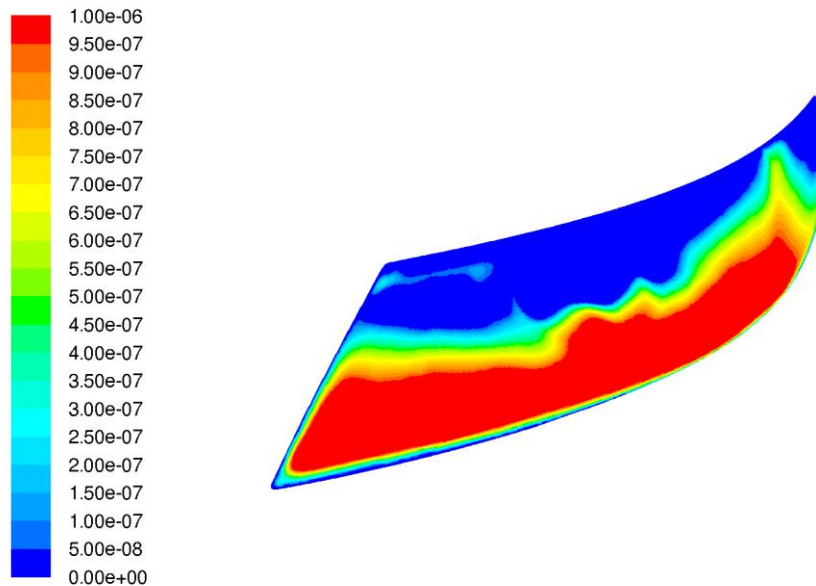


Figure 4.6. Water film thickness [m] on the lens.

As predicted one can see that condensation will form in the lower regions of the outer lens. On the upper regions the film thickness remains zero. When comparing the condensation pattern from the simulation to the climate tunnel test one can also see the expected deviation in the centre of the outer lens, in region C depicted in the Figure below.

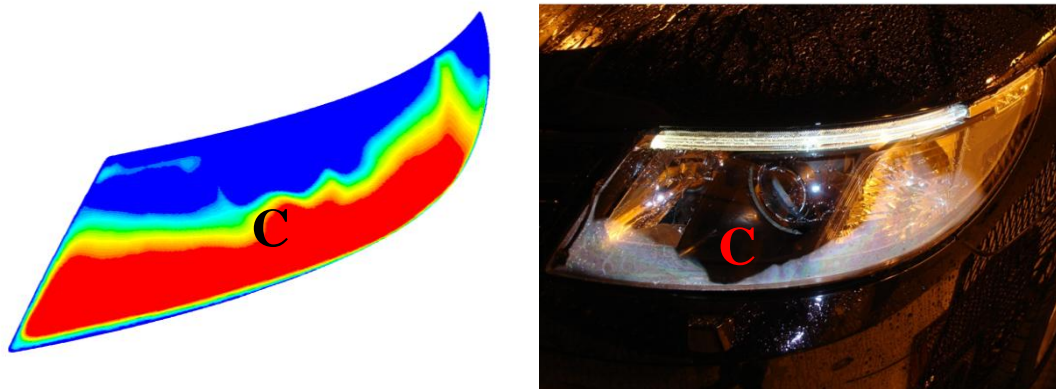


Figure 4.7. Comparison between condensation film thickness patterns for the simulation versus climate tunnel test.

## 5 Conclusion

It has been understood that numerical simulations is a powerful tool to use in the development process. Hence the cost for physical testing can be reduced and the possibilities to make changes early in the development process are large. Although numerical simulations provide these possibilities, it was realized during this thesis that the methodology is not fully optimized. Some areas in the methodology was found to be quite time consuming, more specifically the cad-cleaning and meshing process.

Furthermore a numerical method that predicts if condensation will form on an automotive headlamp was successfully developed. But as stated in Chapter 4 with a deviation according to the results from physical measurements. In order to correct this deviation, further work has to be performed and has been proposed in the next chapter. Also stated was that the main reason for this deviation was found to be in the handling of the settings and boundary conditions for the radiation model. This in turn creates a different temperature distribution on the outer lens compared to the temperature distribution from the physical testing and infrared camera shown in Figures 4.1 and 4.2. Since the condensation pattern is strongly dependent on the temperature distribution on the outer lens one can also understand that the radiation should heat a larger area on the outer lens than what was achieved, thus a larger area of the lens is colder than it should be and thereby more condensation is formed.

The numerical model can therefore not replace physical testing to 100% at this but is on the other hand good enough to be used by CAE Engineers if the proposed recommendations in the next chapter are made.

## 6 Recommendations

In order to take further steps in to decreasing the need for physical testing there needs to be work done both in tweaking the numerical model but also at first adding more measurement points in the already existing physical testing method. This should be done in order to obtain more accurate input data when implementing the boundary conditions. Measurements of interest should conclude radiation through semi-transparent materials, more specifically light distribution behaviour through thick semi-transparent materials for the optical lens.

Another area of interest is the ventilation holes. The simplification made was that the ventilation holes were modelled as pressure outlets with constant atmospheric pressure at both ventilation holes. Earlier reports in [20] states that the influence of these pressures being different due to the difference in height and the vehicle in motion aid the ventilation flow inside the headlamp. This is something that hasn't been looked in to in this thesis and it is strongly recommended to look further in to this, both by physical testing and numerically.

If new and better results are obtained from physical measurements, these can then be used to set more accurate boundary conditions for the numerical model, thus increasing its reliability.

The meshing process is very time consuming and not at all optimized. The internal parts of the headlamp consist of very complex geometry. Tuning the geometry and mesh would probably lead to small changes in the results but could however reduce computational time and data size. Some parts and regions of the headlamp have very little impact on the condensation behaviour and these regions could either be excluded or meshed coarser with larger cell sizes, hence try different software in order to decrease lead time in the pre-processing stage.

In order to capture the correct temperature distribution on the outer lens, settings involving the light distribution through thick semi-transparent materials has to be included and be looked further into. The effect of solar load was not considered in this thesis and may also be necessary to look into.

## 7 References

- [1] H K Versteeg, W Malalasekera, An introduction to Computational Fluid Dynamics – The finite Volume method, second edition, 2007
- [2] The best of Automotive CFD - 3<sup>rd</sup> European Automotive CFD Conference K.W. Seibert, M. Jirka Articles [257, 267].
- [3] Erik Preihs, Automotive headlamp – analytical solution and measurements of condensation inside a headlamp, General Motors, 2006
- [4] Fluent 12, Users Guide
- [5] Fluent 12, Theory Guide
- [6] Sophie Boman, Hanni Shahidi, On the development of a system test-method to evaluate water condensation in automotive headlamps, Master Thesis #3026. Chalmers University Of Technology, Gothenburg, Sweden 2007.
- [7] Yunus A. Cengel, Heat Transfer, A practical approach, second edition. McGraw-Hill, New York, America. p.532
- [8] Incropera/Dewitt/Bergman/Lavine, Fundamental of heat and mass transfer, sixth edition. Wiley.
- [9] Mark Doroudian, Numerical Simulation of Automotive Windshield Defogging. Mindware Engineering, 2002.
- [10] R. B. Kharat, M. R. Nandgaonkar, S. R. Kajale, V. V. Ranade, S. K. Mahajan, 2007, Modeling of in cabin climate and fogging of windshield, SAE world congress Detroit, SAE 2007-01-0767.
- [11] Padmesh Mandloi and Nidhesh Jain, Case-Studies on CFD Simulation of Windshield De-icing. Fluent Corporation, India, 2006.
- [12] R.Arman Dwiartono, Craig W.Somerton, Bashar Abdulnour, Paul Hoke, 2005, The use of numerical simulations to perform engineering calculations of windshield defogging, SAE world congress, Detroit, SAE 2005-01-2054.
- [13] Alberto Deponti, Fabio Damiani, Luca Brugali, Lorenzo Bucchieri, Sergio Zattoni, Jacopo Alaimo, Modelling of condensate formation and disposal inside an automotive headlamp. Published in the Magazine: Engine Soft Newsletter Year 6, no.2.
- [14] Touichirou Shiozawa, Makoto Ohishi, Masatoshi Yoneyama, Koichi Sakakibara, Shuichi, Norihisa Tsuda, Toshio Kobayashi, 2005, Analysis of moisture and natural convection inside an automotive headlamp by using CFD, SAE world congress, Detroit, 2005-01-1449.
- [15] Mike Herridge, 2003, Condensation simulations of automotive lighting assemblies, SAE world congress, Detroit, SAE 2003-01-1211.
- [16] Peter Fischer, 2005, CFD-Analysis and experimental verification of an automotive fog lamp, SAE world congress, Detroit, SAE 2005-01-1921.
- [17] Edinilson Alves Costa, 2006, Wall temperatures and airflow prediction in automotive headlights utilizing the CFD methodology, SAE world congress, Detroit, SAE 2006-01-2646.

- [18] Yoshihiro Okada, Takahide Nouzawa, Takaki Nakamura, CFD Analysis of the flow in an automotive headlamp. Mazda motor company, Hiroshima, Japan, 26 April 2001.
- [19] Bahrenburg, A.W.T, Psychrometry and Psychometric charts, 3<sup>rd</sup> edition, Cape Town, S.A. Cape and Transvaal Printers Ltd., 1974.

## 8 Appendix A

Material properties, for the materials used.

Glass was used as the bulb and the round xenon lens material. Polycarbonate was used as the plastic lens material. Plastic was used on the lightning guide, housing, and all internal frames. Tungsten was used as the filament light source in both the halogen and xenon lamp. Aluminum was used as the material on the reflectors and the xenon frame.

### **Glass:**

Density: 2500 [kg/m<sup>3</sup>]

Specific heat: 830 [J/kgK]

Thermal Conductivity: 1,3 [W/mK]

Absorption Coefficient: 200 [1/m]

Scattering coefficient: 0 [1/m]

Refractive Index: 1,52

### **Plastic:**

Density: 1430 [kg/m<sup>3</sup>]

Specific heat: 1150 [j/kgK]

Thermal Conductivity: 0,52 [W/mK]

Absorption Coefficient: 200 [1/m]

Scattering coefficient: 0 [1/m]

Refractive Index: 1,5

### **Polycarbonate:**

Density: 1200 [kg/m<sup>3</sup>]

Specific heat: 1250 [j/kgK]

Thermal Conductivity: 0,2 [W/mK]

Absorption Coefficient: 200 [1/m]

Scattering coefficient: 0 [1/m]

Refractive Index: 1,58

### **Tungsten:**

Density: 19800 [kg/m<sup>3</sup>]

Specific heat: 24,7 [j/kg×°K]

Thermal Conductivity: 173 [W/m×°K]

Absorption Coefficient: 0 [1/m]

Scattering coefficient: 0 [1/m]

Refractive Index: 1.5

### **Aluminum:**

Density: 2719 [kg/m<sup>3</sup>]

Specific heat: 871 [j/kgK]

Thermal Conductivity: 202,4 [W/mK]

Absorption Coefficient: 200 [1/m]

Scattering coefficient: 0 [1/m]

Refractive Index: 1,5

### **Air:**

Density: -incompressible-ideal-gas- [kg/m<sup>3</sup>]

Specific heat: 1006,43 [j/kgK]

Thermal Conductivity: 0,0242 [W/mK]

Viscosity: 1,789e-05 [kg/ms]

Molecular weight: 28,966 [kg/kgmol]

Absorption Coefficient: 0 [1/m]

Scattering coefficient: 0 [1/m]

Refractive Index: 1